STAT3 signaling in myeloid cells promotes pathogenic myelin-specific T cell differentiation and autoimmune demyelination

Hsueh Chung Lu[a], Sunja Kim[a], Andrew J. Steelman[a,1], Kevin Tracy[b], Beiyan Zhou[c,2], Danielle Michaud[a], Andrew E. Hillhouse[b], Kranti Konganti[b], and Jianrong Li[a,d,3]

[a]Department of Veterinary Integrative Biosciences, Texas A&M University, College Station, TX 77843; [b]Texas A&M Institute for Genome Sciences and Society, Texas A&M University, College Station, TX 77843; [c]Department of Veterinary Physiology and Pharmacology, Texas A&M University, College Station, TX 77843; and [d]Institute for Neuroscience, Texas A&M University, College Station, TX 77843

Edited by Lawrence Steinman, Stanford University School of Medicine, Stanford, CA, and approved January 21, 2020 (received for review August 18, 2019)

Multiple sclerosis (MS) is an autoimmune inflammatory demyelinating disease of the central nervous system. Dysregulation of STAT3, a transcription factor pivotal to various cellular processes including Th17 cell differentiation, has been implicated in MS. Here, we report that STAT3 is activated in infiltrating monocytic cells near active MS lesions and that activation of STAT3 in myeloid cells is essential for leukocyte infiltration, neuroinflammation, and demyelination in experimental autoimmune encephalomyelitis (EAE). Genetic disruption of *Stat3* in peripheral myeloid lineage cells abrogated EAE, which was associated with decreased antigen-specific T helper cell responses. Myeloid cells from immunized *Stat3* mutant mice exhibited impaired antigen-presenting functions and were ineffective in driving encephalitogenic T cell differentiation. Single-cell transcriptome analyses of myeloid lineage cells from preclinical wild-type and mutant mice revealed that loss of myeloid STAT3 signaling disrupted antigen-dependent cross-activation of myeloid cells and T helper cells. This study identifies a previously unrecognized requisite for myeloid cell STAT3 in the activation of myelin-reactive T cells and suggests myeloid STAT3 as a potential therapeutic target for autoimmune demyelinating disease.

multiple sclerosis | myeloid cells | STAT3 signaling | T cell activation | EAE

Functional interactions between the innate and adaptive immune system are pivotal in host defense and must be tightly regulated. In multiple sclerosis (MS), an inflammatory demyelinating disease of the central nervous system (CNS), the involvement of autoreactive T cells in disease pathogenesis is widely recognized (1). Monocytes and macrophages from the innate immune compartment also contribute to neuroinflammation and myelin destruction (2–4). Large-scale genetic studies support both adaptive and innate immune functions in MS pathogenesis (5). In fact, activated macrophages/microglia express antigen-presenting major histocompatibility complex (MHC) class II (6) and are the main inflammatory cells in active MS lesions that often outnumber lymphocytes (7). Variations at the MHC class II locus are the strongest genetic factor for increased MS susceptibility (8). Moreover, peripheral blood mononuclear cells from relapsing remitting MS patients express higher levels of genes involved in antigen processing and inflammation during relapses (9); and genes associated with innate immune cell activation appear overrepresented in progressive MS (10). Although it remains unclear how autoreactive T cells that recognize CNS antigens are activated, myeloid cells likely contribute to MS pathology through their antigen-presenting and innate immune functions.

Experimental autoimmune encephalomyelitis (EAE) is an experimental model that features activation of myelin-reactive lymphocytes and infiltration of immune cells leading to meningitis, inflammatory demyelination, and axonal damage in the CNS, key pathological components of MS, and is thus commonly used to model autoimmune demyelination aspects of MS. In EAE, monocytic cells represent a prominent component of neuroinflammatory infiltrates and have been shown to be crucial for facilitating T cell polarization, immune cell invasion, and disease pathogenesis (11–16). As EAE is largely driven by autoreactive T helper (Th) cells, myeloid cells are necessary for EAE due to both their role in differentiating T cells into Th1 and Th17 subsets in the peripheral lymphatic organs and their ability to reactivate them within the CNS. Interactions between autoreactive T cells and antigen-presenting cells (APCs) perpetuate local CNS autoimmune reactions and drive disease progression (17). Furthermore, APCs directly interact with effector T cells during EAE in leptomeninges and nascent CNS lesions (18, 19). As such, it is perhaps not surprising that increases in circulating inflammatory monocytes correlate with relapses (20). However, intracellular mechanisms that drive myeloid cell activation of T cells during CNS autoimmunity remain incompletely understood.

Significance

Myeloid lineage cells are suspected of having an integral role in pathophysiological processes of multiple sclerosis (MS), but the molecular mechanism(s) governing their effector function remains incompletely understood. We show that STAT3 is activated in myeloid cells near active MS lesions. Conditional deletion of *Stat3* in myeloid cells abolished symptoms of experimental autoimmune encephalomyelitis (EAE) by suppressing the generation of pathogenic T cells. Functional and transcriptomic analyses of myeloid cells from wild-type and conditional knockout mice implicated antigen processing/presentation and inflammatory cytokine production as the mechanism underlying the effects of STAT3 deletion on impaired T cell activation. Our data indicate that targeting STAT3 in myeloid cells might be a viable treatment option for autoimmune demyelinating disease.

Author contributions: H.C.L. and J.L. designed research; H.C.L., S.K., A.J.S., D.M., A.E.H., and J.L. performed research; H.C.L., S.K., K.T., B.Z., K.K., and J.L. analyzed data; and H.C.L. and J.L. wrote the paper.

The authors declare no competing interest.

This article is a PNAS Direct Submission.

This open access article is distributed under Creative Commons Attribution-NonCommercial-NoDerivatives License 4.0 (CC BY-NC-ND).

Data deposition: The sequence reported in this paper has been deposited in the National Center for Biotechnology Information (NCBI) BioProject database (accession no. PRJNA605403).

[1]Present address: Department of Animal Sciences, University of Illinois at Urbana–Champaign, Urbana, IL 61801.

[2]Present address: Department of Immunology, University of Connecticut Health Center, Farmington, CT 06030.

[3]To whom correspondence may be addressed. Email: jrli@cvm.tamu.edu.

This article contains supporting information online at https://www.pnas.org/lookup/suppl/doi:10.1073/pnas.1913997117/-/DCSupplemental.

First published February 24, 2020.

Signal transducer and activator of transcription 3 (STAT3), a member of the Janus kinase (JAK)/STAT family of tyrosine kinases, transduces extracellular signals from cytokines such as interleukin (IL)-6 and IL-10 and regulates an array of genes critical for immune responses and cell differentiation (21). Genome-wide association studies identified *Stat3* as a potential MS susceptibility locus (22–25); however, the exact role of STAT3 in MS pathogenesis is not clear. Elevated levels of phosphorylated STAT3 have been found in circulating T cells and monocytes from MS patients and correlate with disease progression (26–28). Phosphorylated STAT3 was also observed in macrophages/microglia and astrocytes in the white matter adjacent to active MS lesions (29). Mice with selective deletion of the *Stat3* gene in $CD4^+$ T cells did not develop EAE due to impaired induction of encephalitogenic Th17 cells (30). Systemic blockade of JAK/STAT pathways suppressed Th1/Th17 differentiation, myeloid cell activation, and leukocyte infiltration during EAE (31). Conversely, STAT3 appears to have a nonredundant role in IL-10–mediated antiinflammatory responses in monocytes/macrophages as *Il10* deficiency results in exacerbated EAE (32). Therefore, loss of *Stat3* in myeloid cells may aggravate inflammation and autoimmune diseases. On the other hand, STAT3 mediates IL-6 signaling, and *Il6*-null mice are resistant to EAE due to deficiency of effector T cell development (33–35). Interestingly, myeloid cell-specific ablation of *Socs3,* a negative regulator of STAT3, results in excessive Th1/17 responses and exacerbated demyelination of the cerebellum (36), underscoring a potential pathogenic role for STAT3 overactivation in myeloid cells in neuroinflammation.

To determine the in vivo function of myeloid STAT3 signaling in CNS autoimmune diseases, we generated myeloid cell-restricted *Stat3* mutant mice and subjected them to $MOG_{35–55}$-induced EAE. Here, we provide in vivo evidence that activation of STAT3 in peripheral myeloid cells is required for EAE development in large part through cross-talk with $CD4^+$ T cells and promotion of Th1/Th17 cell differentiation and activation.

Results

STAT3 Is Activated in Subsets of $CD11b^+$ Cells Adjacent to Active MS Lesions and in Inflamed Loci in the EAE Animal Model of MS. As the transcriptional activity of STAT3 is critically dependent on phosphorylation of tyrosine 705 (pY705), the levels of phosphorylated STAT3 (pSTAT3, Y705) and total STAT3 were evaluated by Western blotting analysis of postmortem brain tissues from MS patients and control subjects (Fig. 1 *A* and *B* and *SI Appendix*, Table S1). We found significant increases in both pSTAT3 (~4.9-fold) and total STAT3 (~2.3-fold) in MS tissues compared to controls (Fig. 1*B*). Cellular location of pSTAT3 was then determined by double immunolabeling with monoclonal antibodies that specifically detect STAT3 phosphorylated at Tyr705. While we did not find a pSTAT3 signal in control cases, we observed sparse pSTAT3-positive cells near demyelinating lesions in the white matter (Fig. 1*C*). Most interestingly, we often observed distinct pSTAT3 immunoreactivity in $CD11b^+$ monocytes in the lumen of blood vessels and perivascular regions (Fig. 1*D*). Similarly, STAT3 immunoreactivity was elevated in macrophages/microglia clustered around blood vessels (Fig. 1*E*), a finding consistent with the vasocentric nature of new lesion formation that is often seen in MS. These findings demonstrate that not only total STAT3 expression is increased, it is also activated in subsets of myeloid cells that are frequently associated with the inflamed vasculature in active MS, and suggest that myeloid STAT3 activation may be involved in the pathogenesis of new lesion formation.

Next, we investigated whether STAT3 is activated in the EAE model of MS as EAE approximates autoimmune activation and cell trafficking aspects of MS. In contrast to a complete lack of pSTAT3 immunoreactivity in normal spinal cords (Fig. 2*A*), prominent pSTAT3 immunoreactivity was found at the site of immune cell infiltration in EAE mice (Fig. 2 *B*–*F*). Using a visual method for colocalization, in which colocalization is determined if a cell or its nucleus exhibits yellow color when the green (cell markers) and red (pSTAT3) channels are superimposed, we found that pSTAT3 signal was colocalized to a subset of $CD68^+$ (Fig. 2*C*), tomato $lectin^+$ (Fig. 2*D*), and $CD11b^+$ myeloid cells (Fig. 2*E*). Very few $pSTAT3^+$ cells were $GFAP^+$ astrocytes (Fig. 2*B*) or $CD4^+$ T cells (Fig. 2*F*). This spatial distribution of $pSTAT3^+$ cells further suggests that STAT3 activation in myeloid cells may contribute to immune cell infiltration and the pathogenesis of EAE.

Selective Ablation of *Stat3* in Myeloid Cells Abrogates $MOG_{35–55}$-Induced EAE. To investigate the in vivo function of myeloid STAT3 in autoimmune demyelination, we disrupted *Stat3* gene specifically in myeloid lineage cells. *Stat3* gene was floxed at exon 22 encoding the Tyr residue that is essential for STAT3 activation (37) (Fig. 3*A*). Truncated STAT3 protein may be expressed but is not activated due to the lack of Tyr705, resulting in functional STAT3 inactivation in targeted cells. We confirmed that the targeted sequence of *Stat3* gene was indeed deleted upon recombination as determined by genomic PCR of fluorescence-activated cell sorting (FACS) isolated $CD11b^+$ splenocytes (Fig. 3*B*). Flow cytometry analysis of *LysMcre* reporter mice (*LysMcre:rosa26-Ai14*) further showed high efficacy of cre recombination in peripheral myeloid cells, such as granulocytes, $Ly6C^{hi}$ and $Ly6C^{lo}$ monocytes, and dendritic cells, but not CNS microglia (*SI Appendix*, Fig. S1*C*). In addition, IL-6–induced STAT3 phosphorylation was markedly abolished in bone marrow-derived macrophages (BMDMs) from *LysMcre:Stat3*$^{fl/fl}$ in comparison to controls (*SI Appendix*, Fig. S1).

LysMcre:Stat3$^{fl/fl}$ and littermate *Stat3*$^{fl/fl}$ controls were then subjected to $MOG_{35–55}$-induced EAE. In stark contrast to *Stat3*$^{fl/fl}$ mice that developed typical EAE symptoms and progression, *LysMcre:Stat3*$^{fl/fl}$ mice were resistant (Fig. 3 *C* and *D*) and did not exhibit characteristic weight loss associated with EAE onset (Fig. 3*E*). Consistent with the lack of EAE symptoms in the *LysMcre:Stat3*$^{fl/fl}$ mice, there was little peripheral immune cell infiltration (Fig. 3 *G* and *H*), microglia activation (Fig. 3 *I* and *J*), and demyelination (Fig. 3*F*). Although activated $CD68^+$ macrophages were present in leptomeninges of the *LysMcre:Stat3*$^{fl/fl}$ mice, they were essentially excluded from CNS parenchyma (Fig. 3*I*). Moreover, *LysMcre:Stat3*$^{fl/fl}$ mice also had attenuated spinal production of proinflammatory cytokines (*Tnf, Il1β, Ifnγ*, and *Gm-csf*) and chemokines (*Ccl2, Ccl3*, and *Ccl5*) compared to controls (Fig. 3*K*). EAE-associated up-regulation of intercellular adhesion molecule-1 (*Icam-1*) and loss of activated leukocyte cell adhesion molecule (*Alcam*) were also abolished in *LysMcre:Stat3*$^{fl/fl}$ mice (*SI Appendix*, Fig. S2*A*). Immunohistochemistry confirmed robust up-regulation of ICAM-1 in immunized *Stat3*$^{fl/fl}$ mice, particularly in regions where leukocytes infiltrated, whereas moderate ICAM-1 immunoreactivity in the mutant mice was largely restricted to leptomeninges (*SI Appendix*, Fig. S2). Taken together, these data demonstrate that disruption of STAT3 signaling in myeloid cells abrogated EAE development and prevented leukocyte infiltration, neuroinflammation, and demyelination.

Peripheral Antigen-Specific Th1 Responses Are Reduced in *Stat3* Mutant Mice at the Preclinical and Onset Stages of EAE. To determine if the lack of CNS inflammatory responses in *LysMcre:Stat3*$^{fl/fl}$ mice was resulted from impaired development of encephalitogenic Th1/Th17 cells, we examined the kinetics of antigen-specific T cell responses over the course of EAE. Mononuclear cells were isolated from secondary lymphatic organs of immunized mice at different stages of EAE and tested for their responses upon secondary exposure to $MOG_{35–55}$ peptide (Fig. 4). During the preclinical and onset stages of EAE, *LysMcre:Stat3*$^{fl/fl}$ splenocytes secreted significantly less interferon (IFN) γ (Fig. 4*A*) and a

IMMUNOLOGY AND INFLAMMATION

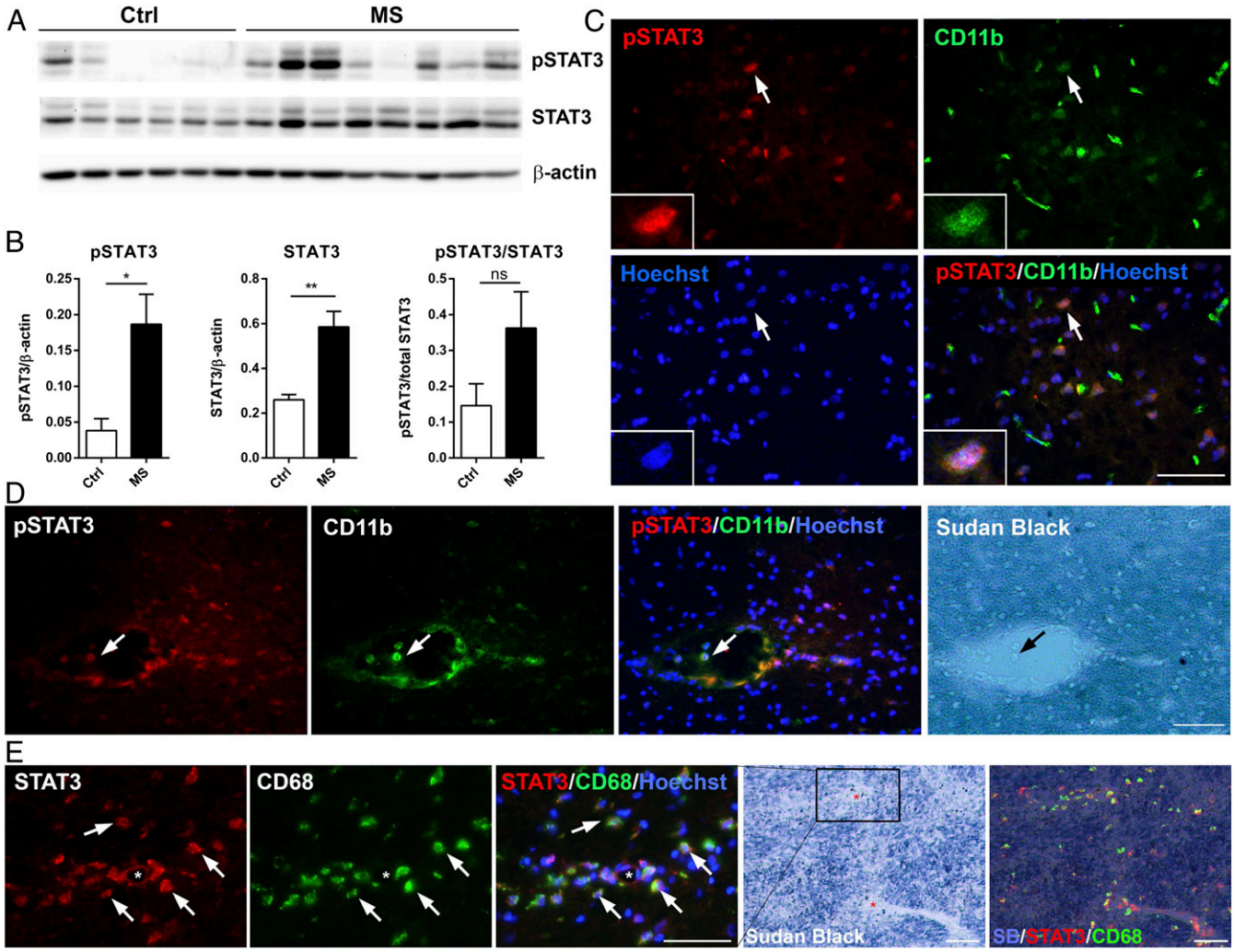

Fig. 1. Increased STAT3 phosphorylation in myeloid cells in MS. (*A* and *B*) Western blot and densitometry analysis of brain white matter tissue lysates from nonneurological controls ($n = 6$) and MS patients ($n = 8$) with antibodies against pSTAT3 (Y705) and total STAT3. Data represent mean ± SEM; $^{*}P < 0.05$; $^{**}P < 0.01$; ns, not significant. (*C*) Representative photomicrographs of double-immunostained MS brain tissues showing pSTAT3 (Y705) in subsets of $CD11b^{+}$ cells in the white matter lesions. (*D*) Representative images depicting $pSTAT3^{+}$ $CD11b^{+}$ double-positive cells in the lumen of a blood vessel and perivascular space in the normal appearing white matter from a progressive MS case. Myelin was labeled with Sudan black. (*E*) Representative images showing spatial distribution of STAT3 immunoreactivity to $CD68^{+}$ activated macrophages/microglia around small blood vessels of a chronic progressive MS case. (Scale bars: 50 μm.)

trend of less IL-17A (Fig. 4*B*) when compared to littermate controls. Moreover, antigen-elicited production of the pathogenic cytokine granulocyte-macrophage colony-stimulating factor (GM-CSF) was significantly suppressed in the mutant mice compared to littermate controls at the onset of disease (Fig. 4*C*). Consistent with these data, the frequency (Fig. 4 *D–H*) and the number (*SI Appendix*, Fig. S4) of IFNγ- and GM-CSF–producing $CD4^{+}$ T cells were significantly lower in immunized *LysMcre:Stat3*$^{fl/fl}$ mice than that of *Stat3*$^{fl/fl}$ mice at disease onset. In contrast to diminished pathogenic T cell responses during the early phase of EAE, antigen-specific production of IFNγ, GM-CSF, IL-17A, and many proinflammatory mediators was comparable between genotypes at later stages (Fig. 4 *A–C* and *SI Appendix*, Fig. S3). Major myeloid and lymphocyte populations in blood and spleens were also similar between genotypes (*SI Appendix*, Fig. S5). Collectively, these data show that disruption of STAT3 signaling in myeloid cells results in decreased pathogenic Th1 responses, primarily at preclinical and early stages of EAE, and that activation of STAT3 in myeloid cells is required for generating antigen-specific encephalitogenic $CD4^{+}$ T helper cells and induction of EAE.

Disruption of STAT3 Signaling in Myeloid Cells Impairs Their Capability to Differentiate Naive $CD4^{+}$ T Cells into Th1 and Th17 Ex Vivo. Direct engagement of naive $CD4^{+}$ T cells with antigen-presenting cells and a proper cytokine milieu dictate the differentiation of T cells into effector cells. To directly test whether *Stat3* mutant myeloid cells are less efficient at differentiating naive $CD4^{+}$ T cells into antigen-specific pathogenic T cells, we took an ex vivo coculture approach (Fig. 5*A*). We isolated $CD11b^{+}$ splenocytes from *LysMcre:Stat3*$^{fl/fl}$ and littermate *Stat3*$^{fl/fl}$ mice 9 d after immunization with $MOG_{35–55}$ and cocultured them with $CD4^{+}$ T cells from naive 2D2 mice that express a transgenic TCR for $MOG_{35–55}$ (38) (Fig. 5*A*). Positive immunomagnetic selection for CD11b and CD4 yielded highly enriched corresponding populations (*SI Appendix*, Fig. S6 *A* and *B*), and immunophenotyping analyses revealed no overt populational differences in isolated $CD11b^{+}$ cells between genotypes (*SI Appendix*, Fig. S6*C*). However, upon culturing with naive $CD4^{+}$ 2D2 T cells in the presence of $MOG_{35–55}$, the cocultures containing *Stat3* mutant myeloid cells had a lower percentage of $CD11b^{+}CD11c^{+}$ APCs than that with wild-type (WT) myeloid cells (*SI Appendix*, Fig. S6*D*), and fewer IFNγ- and IL-17A–producing $CD4^{+}$ T cells (Fig. 5*B*). Consistent with decreased

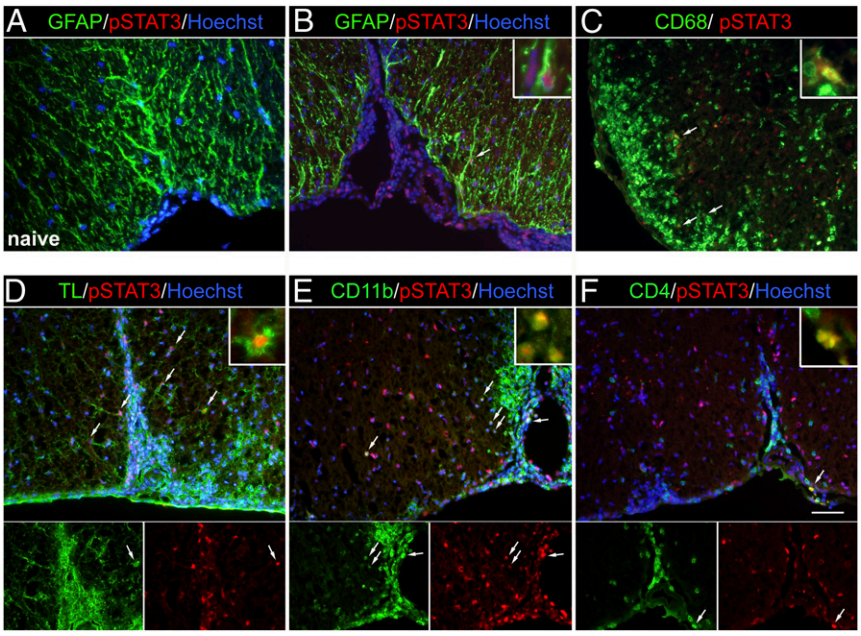

Fig. 2. STAT3 is activated in infiltrating myeloid cells during the peak of EAE. Spinal cord sections from normal naive mice and EAE mice at 14 d post-immunization (dpi) (clinical score 2 to 3) were analyzed by immunofluorescence microscopy. Representative images of medial ventral spinal cord areas are shown. Arrows indicate double-positive cells. (*A*) pSTAT3 was not detected in spinal cord sections from normal mice. (*B* and *C*) Colocalization of pSTAT3 to a few GFAP$^+$ astrocytes and CD68$^+$ activated microglia/macrophages during EAE. (*Inset*) Higher magnification of double-labeled cells. (*D*) Some pSTAT3$^+$ cells were also positive for tomato lectin (TL) that labels blood vessels and microglia/macrophages. (*E*) Colocalization of pSTAT3 to CD11b$^+$ cells. (*F*) pSTAT3$^+$ cells in the parenchyma rarely were CD4$^+$. The arrow indicates a pSTAT3$^+$CD4$^+$ T cell found in the leptomeninges of EAE mice. (Scale bar: 50 μm.)

number of Th1 and Th17 cells in MOG-stimulated mutant myeloid cells plus 2D2 T cells, antigen-specific production of IFNγ, IL-17A, and GM-CSF was also significantly reduced (Fig. 5*C*). Many other inflammatory mediators, including TNFα, IL-1β, IL-6, IL-12, IL-4, IL-18, IL-23, CCL3, and CCL5, were similarly reduced in cocultures of 2D2 T cells with mutant myeloid cells (*SI Appendix*, Fig. S7*A*). Furthermore, mutant CD11b$^+$ cells were less efficient than their wild-type counterpart in promoting Th1 cell proliferation (*SI Appendix*, Fig. S8). Together, these data suggest that myeloid cells from immunized *LysMcre:Stat3$^{fl/fl}$* mice are less efficient in polarizing and activating Th1 and Th17 cells and eliciting antigen-specific adaptive immune responses.

In the absence of T cells, CD11b$^+$ cells from immunized *LysMcre:Stat3$^{fl/fl}$* mice produced lower levels of TNFα and IL-1β than that of *Stat3$^{fl/fl}$* mice upon lipopolysaccharide (LPS)/IFNγ activation (Fig. 5*D*). We also observed decreased production of IL-17A, CCL3, and CCL5, but not IL-6, IL-12, IL-4, IL-10, IL-18, IL-23, or IP-10 upon LPS/IFNγ activation (Fig. 5*D* and *SI Appendix*, Fig. S7*B*). In contrast, CCL2 was significantly higher in stimulated mutant CD11b$^+$ monocultures (*SI Appendix*, Fig. S7*B*). Interestingly, mutant myeloid cells expressed significantly less MHC class II than wild-type cells upon stimulation (Fig. 5*E* and *SI Appendix*, Fig. S9). The decreased expression of MHC class II and costimulatory molecules on mutant myeloid cells may account for decreased antigen-specific Th1/Th17 responses in cocultures, which in turn produced less instructive signals, such as GM-CSF to myeloid cells, resulting in decreased myeloid cell activation and production of proinflammatory cytokines.

To examine whether inactivation of STAT3 affects individual myeloid cell types differentially, we stimulated ex vivo CD11b$^+$ cells (Fig. 5*A*) with LPS and examined TNFα production in individual cells by intracellular staining and flow cytometry (*SI Appendix*, Fig. S10). When compared to wild-type cells, a lower percentage of mutant Ly6C^{hi} and Ly6C^{low} monocytes produced TNFα upon activation, in agreement with above multiplex findings (Fig. 5 and *SI Appendix*, Fig. S7). Although there was no difference in TNFα production between mutant and wild-type neutrophils, we found a significant reduction in MOG-dependent secretion of myeloperoxidase (MPO) in the *Stat3* mutant myeloid cocultures (*SI Appendix*, Fig. S10*B*), suggesting that neutrophil activation may be affected by the loss of STAT3 signaling.

Previous study showed that *Stat3*-deficient peritoneal macrophages exhibit enhanced proinflammatory responses due to loss of the IL-10/STAT3 antiinflammatory axis (39). Therefore, we examined BMDMs from naive *LysMcre:Stat3$^{fl/fl}$* and littermate controls. While differentiation and maturation of BMDMs were comparable between genotypes (*SI Appendix*, Fig. S11*A*), upon stimulation, *LysMcre:Stat3$^{fl/fl}$* BMDMs expressed lower levels of CD40 and CD80, higher MHC class II, and proinflammatory mediators such as TNFα, IL-1β, IL-6, IL-12, and CCL2 at both messenger RNA (mRNA) and protein levels than control BMDMs (*SI Appendix*, Fig. S11 *B–D*). In cocultures of BMDM plus Th1 or Th17 cells, antigen-specific production of IFNγ and IL-17A was not different between genotypes (*SI Appendix*, Fig. S11*E*). Our results confirmed previous findings that STAT3-deficient macrophages exhibit enhanced innate immune responses but, in the meantime, revealed that cultured BMDMs did not recapitulate immune responses of myeloid cells isolated from MOG-immunized mice (Fig. 5 and *SI Appendix*, Fig. S7), which further underscores the importance of examining STAT3-dependent immune responses in vivo.

***LysMcre:Stat3$^{fl/fl}$* Mice Develop Passive EAE after Adoptive Transfer of Encephalitogenic T Cells.** Our data thus far suggest that impaired development of myelin-specific Th1 underlies the insensitivity of *Stat3* mutant mice to MOG$_{35–55}$-induced EAE. If this indeed is the case, *LysMcre:Stat3$^{fl/fl}$* mice should be susceptible to passive EAE mediated by adoptive transfer of encephalitogenic T cells (Fig. 6*A*). After antigen reactivation, donor cells from draining lymph nodes of preclinical EAE mice consisted primarily of B cells, CD8$^+$ T cells, and CD4$^+$ T cells, of which 46.6% were IFNγ-secreting Th1 and 32.4% were IL-17A–secreting Th17 cells (*SI Appendix*, Fig. S12 *A* and *B*). In contrast to active EAE, where only about 5% of *LysMcre:Stat3$^{fl/fl}$* mice developed the disease (Fig. 3), two-thirds of the mutant mice developed passive EAE after receiving encephalitogenic T cells (Fig. 6), and ones that developed disease had comparable levels of neuroinflammation as wild-type controls (Fig. 6 *D–F* and *SI Appendix*, Fig. S12*C*). These data further support the notion that myeloid STAT3 signaling is critical to the development of myelin-specific pathogenic T cells.

It is worth noting that, although a majority of *LysMcre:Stat3$^{fl/fl}$* mice developed EAE symptoms upon adoptive transfer of encephalitogenic T cells, their overall clinical scores were lower

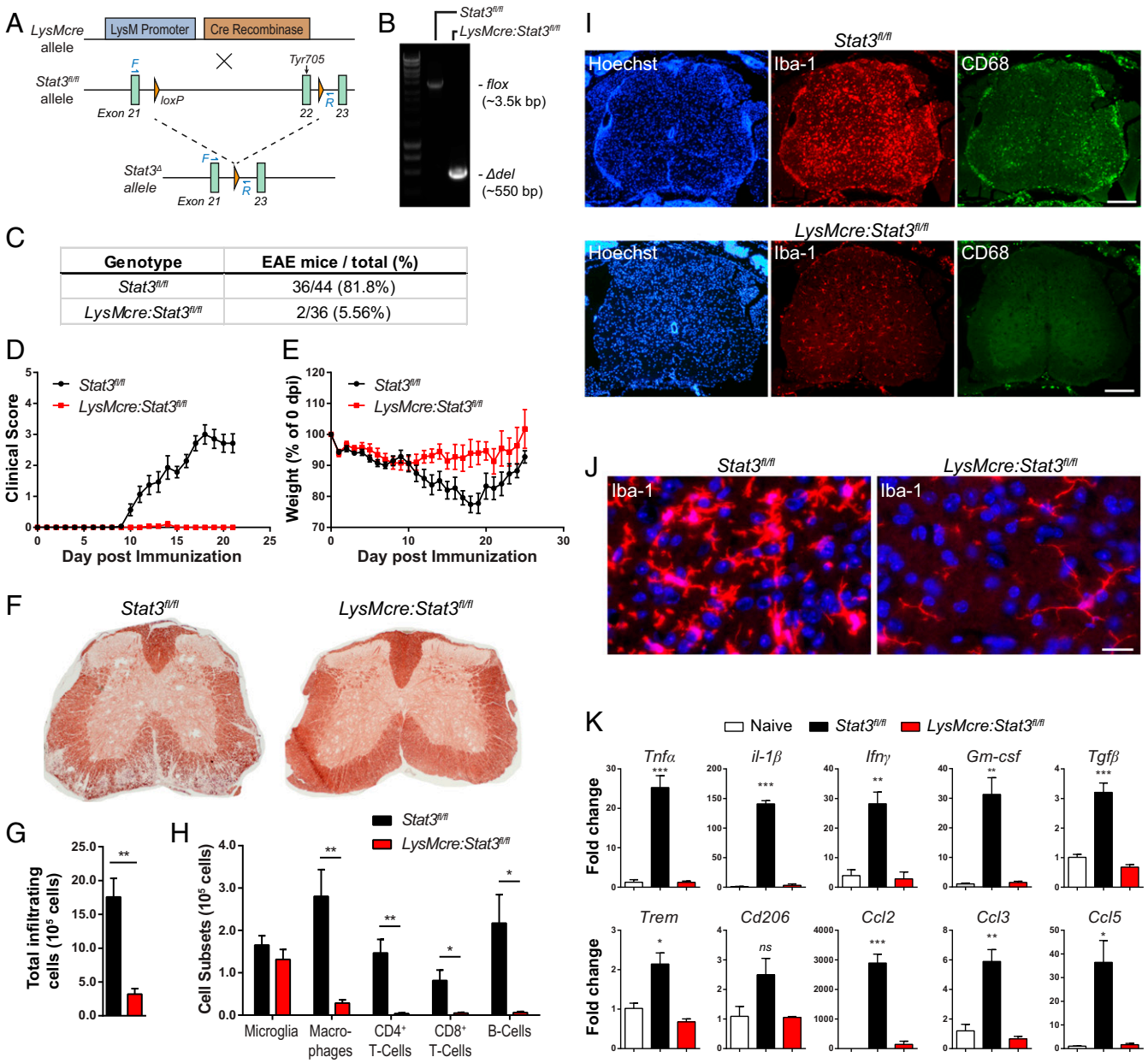

Fig. 3. Mice with targeted disruption of *Stat3* in myeloid cells are resistant to MOG_{35-55}-induced EAE. (*A*) Schematic of Cre-dependent excision of exon 22 of *Stat3* gene that encodes tyrosine 705 residue essential for STAT3 protein activation. F and R depict forward and reverse primers designed to flank the entire deleted sequence (forward-CCTCTACCCCGACATTCCCAAGG; reverse-CACACAAGCCATCAAACTCTGGTCTC). (*B*) *Stat3* deletion efficiency in $CD11b^+$ cells FACS-sorted from the spleens of *LysMcre:Stat3*$^{fl/fl}$ and *Stat3*$^{fl/fl}$ mice. Genomic PCR was used to amplify the floxed region (~3,500 base pairs [bp]) and truncated *Stat3* (Δdel; ~550 bp). (*C–E*) *Stat3*$^{fl/fl}$ (n = 44) and *LysMcre:Stat3*$^{fl/fl}$ mice (n = 36) were subjected to MOG_{35-55}-induced EAE and scored daily. Table of percentage of mice with EAE disease (*C*), mean EAE clinical scores (*D*), and percentage body weight changes over time (*E*). Data represent eight independent experiments. (*F*) Representative myelin staining of EAE mice at 21 d post-immunization (dpi). (*G* and *H*) Flow cytometry analyses of mononuclear cells isolated from the CNS of *Stat3*$^{fl/fl}$ (n = 4) and *LysMcre:Stat3*$^{fl/fl}$ EAE mice (n = 4) at 14 dpi. Immunized *LysMCre:Stat3*$^{fl/fl}$ mice had significantly fewer leukocyte infiltrates (*G*), macrophages ($CD11b^+CD45^{hi}$), and T cells and B cells in the CNS while microglia population ($CD11b^+CD45^{int}$) were similar between genotypes (*H*). (*I* and *J*) Representative images of spinal cord lumbar sections from EAE mice at 21 dpi stained for Iba-1, CD68, and Hoechst. (Scale bars: *I*, 200 μm; *J*, 20 μm.) (*K*) Quantitative RT-PCR analysis of spinal cords isolated from *Stat3*$^{fl/fl}$ (n = 5) and *LysMcre:Stat3*$^{fl/fl}$ mice (n = 5) at 14 dpi. Data represent fold changes relative to naive mice (n = 3) and are mean ± SEM. $^*P < 0.05$, $^{**}P < 0.01$, $^{***}P < 0.005$ as determined by one-way ANOVA. ns, not significant.

than that of *Stat3*$^{fl/fl}$ mice, which suggests additional mechanisms or cell types affected by loss of myeloid STAT3 signaling. One possibility is impaired innate functions of mutant macrophages and neutrophils (*SI Appendix*, Fig. S10).

STAT3 Activation in the Peripheral Myeloid Cells, but Not CNS Microglia, Is Necessary for the Development of Active EAE. Our data above suggest that STAT3 activation in blood-derived myeloid cells plays a pathogenic role in the induction of EAE. To address whether *LysMcre:Stat3*$^{fl/fl}$ mice become susceptible to MOG-induced EAE when their peripheral myeloid cells are replenished with wild-type cells as well as whether CNS microglial STAT3 contributes to EAE pathogenesis, we generated bone-marrow (BM) chimeric mice (Fig. 7*A*). Flow cytometry analyses of splenocytes, blood, and CNS mononuclear cells from chimeric mice showed high engraftment efficiency of the peripheral

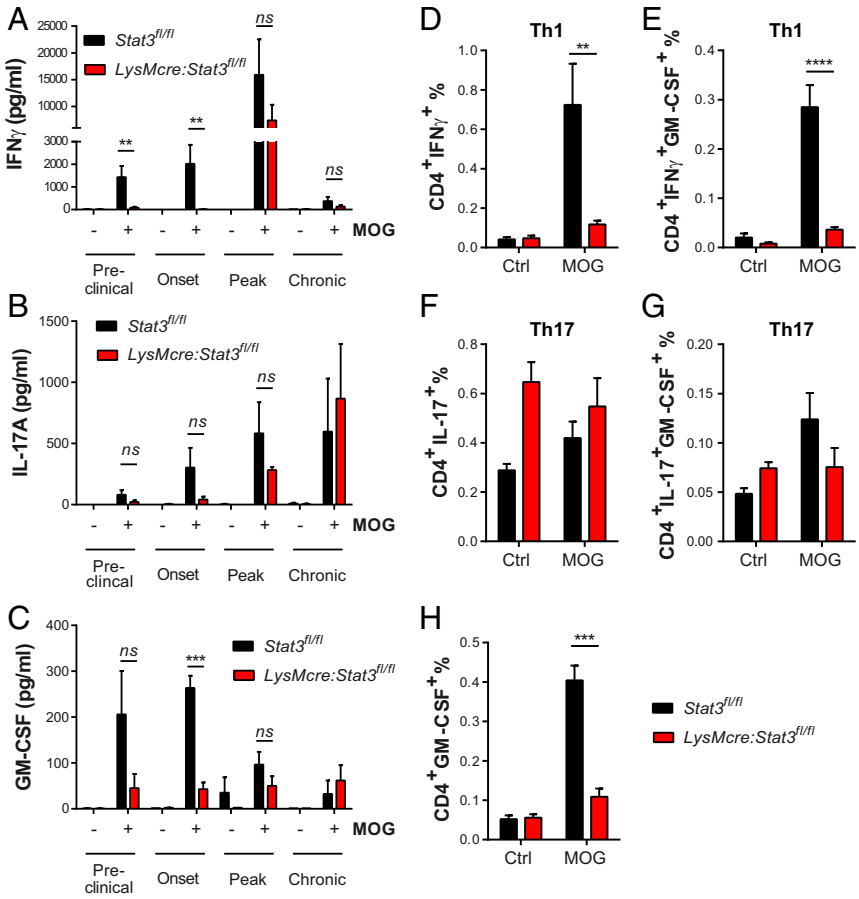

Fig. 4. Peripheral antigen-specific T cell responses were impaired in myeloid *Stat3* mutant mice during preclinical and onset of EAE. (*A–C*) EAE was induced in *LysMcre:Stat3*$^{fl/fl}$ and *Stat3*$^{fl/fl}$ control mice. At different EAE stages based on clinical scores of control *Stat3*$^{fl/fl}$ mice, splenocytes were isolated and cultured in the absence or presence of $MOG_{35–55}$ (30 μg/mL) for 3 d. Production of IFNγ, IL-17A, and GM-CSF in the supernatant was determined with ELISA. Preclinical, *Stat3*$^{fl/fl}$, $n = 6$; *LysMcre:Stat3*$^{fl/fl}$, $n = 5$. Onset, *Stat3*$^{fl/fl}$, $n = 6$; *LysMcre:Stat3*$^{fl/fl}$, $n = 4$. Peak, *Stat3*$^{fl/fl}$, $n = 5$; *LysMcre:Stat3*$^{fl/fl}$, $n = 2$. Post-peak, *Stat3*$^{fl/fl}$, $n = 3$; *LysMcre:Stat3*$^{fl/fl}$, $n = 2$. Data represent mean ± SEM. $^{**}P < 0.01$, $^{***}P < 0.005$. (*D–H*) Intracellular cytokine analysis of the frequency of IFNγ-, IL-17A-, and GM-CSF-producing $CD4^+$ effector T cells. Splenocytes were isolated at disease onset and rechallenged with antigen $MOG_{35–55}$ for 24 h. Intracellular cytokine production by $CD4^+$ T cells was analyzed by flow cytometry after secretion blockade with Brefeldin A followed by immunostaining with fluorophore-conjugated antibodies against CD4, IFNγ, IL-17A, and GM-CSF. *Stat3*$^{fl/fl}$, $n = 6$; *LysMcre:Stat3*$^{fl/fl}$, $n = 4$. Data represent mean ± SEM; ns, not significant; $^{**}P < 0.01$, $^{***}P < 0.005$, $^{****}P < 0.001$.

immune system (85 to 95%) and minimal engraftment in the CNS (Fig. 7*B*). Moreover, chimera reconstituted with BM from *LysMcre:Rosa*^{tdTomato} reporter mice confirmed that peripheral myeloid cells do not engraft into the CNS parenchyma under normal conditions (Fig. 7*C*). The few tdTomato$^+$ (tdT$^+$) donor cells found per tissue section were all associated with meninges or blood vessels. In contrast, when *Cx3cr1*$^{gfp/+}$ transgenic mice, in which microglia express GFP, were reconstituted with *LysMcre:Rosa*^{tdTomato} BM and later subjected to EAE, massive peripheral donor-derived tdTomato$^+$ myeloid cells infiltrated into the CNS and were clearly distinguishable from resident GFP$^+$ microglia (Fig. 7*D*). These results show that peripheral infiltrates are the primary driver of neuroinflammation and that the chimera model is suitable for investigating central and peripheral immune contributions in EAE. *Stat3*$^{fl/fl}$ chimeric mice were then examined for their susceptibility to MOG-induced EAE. Chimeric mice engrafted with wild-type BM (i.e., *Stat3*$^{fl/fl}$ (donor) → *Stat3*$^{fl/fl}$ (recipient) and *Stat3*$^{fl/fl}$ → *LysMcre:Stat3*$^{fl/fl}$) developed typical EAE (Fig. 7 *E* and *F*). In contrast, chimeric mice hosting mutant myeloid cells in the periphery (i.e., *LysMcre:Stat3*$^{fl/fl}$ → *Stat3*$^{fl/f}$ and *LysMcre:Stat3*$^{fl/fl}$ → *LysMcre:Stat3*$^{fl/f}$) failed to develop EAE (Fig. 7 *E* and *F*). In line with clinical scores, the number of CNS infiltrates were indistinguishable between wild-type and mutant mice that received wild-type BM (Fig. 7 *G* and *H*), suggesting that STAT3 activation in the peripheral myeloid compartment, but not the CNS compartment, is critical for the development of EAE.

During our EAE experiments involving bone marrow chimeric mice, we observed that, although wild-type mice reconstituted with mutant BM (*LysMcre:Stat3*$^{fl/fl}$ → *Stat3*$^{fl/fl}$) did not develop EAE (Fig. 7*D*), they displayed sickness behaviors, appeared hunched and lethargic, and died at various days after MOG immunization. These mice, however, did not develop other symptoms associated with atypical EAE, such as ataxia and axial rotation. We suspect this may due to enhanced innate immune responses elicited by immunization as we found that the serum from *LysMcre:Stat3*$^{fl/fl}$ mice at the preclinical stage had higher levels of TNFα compared to littermate controls and that STAT3-deficient BMDMs had exacerbated immune responses upon LPS stimulation (*SI Appendix*, Fig. S11). Of note, *LysMcre:Stat3*$^{fl/fl}$ → *Stat3*$^{fl/fl}$ chimeric mice did not exhibit any apparent health problems prior to immunization. *LysMcre:Stat3*$^{fl/fl}$ → *LysMcre:Stat3*$^{fl/fl}$ chimeric mice did not exhibit these problems, probably due to inherent adaptation to myeloid *Stat3* inactivation.

To overcome the adverse effects of myeloablation by irradiation and to determine the contribution of microglial STAT3, we generated tamoxifen-inducible microglia-specific *Stat3* mutant mice. The efficiency of *Cx3cr1*-driven recombination in microglia (40) was first established with reporter mice (Fig. 8 *A–C*). Although recombination occurred in peripheral CX_3CR_1-expressing cells (Fig. 8*C*), 4 wk after tamoxifen pulse treatment, the short-lived blood-born Cx3cr1-expressing cells were replaced by unrearranged bone marrow progeny whereas Cre-recombined microglia persisted (>96%), resulting in specific gene targeting in long-lived microglial cells (Fig. 8*C*). When active EAE was induced in *Stat3*$^{fl/fl}$ and *Cx3cr1*$^{CreERT:}$*Stat3*$^{fl/fl}$ mice 4 wk after tamoxifen treatment, EAE clinical scores (Fig. 8 *D* and *E*) and CNS cytokine transcripts (Fig. 8*F*) were not significantly different between genotypes. Thus, our collective data demonstrate that microglia STAT3 signaling does not play a major role in EAE development and progression.

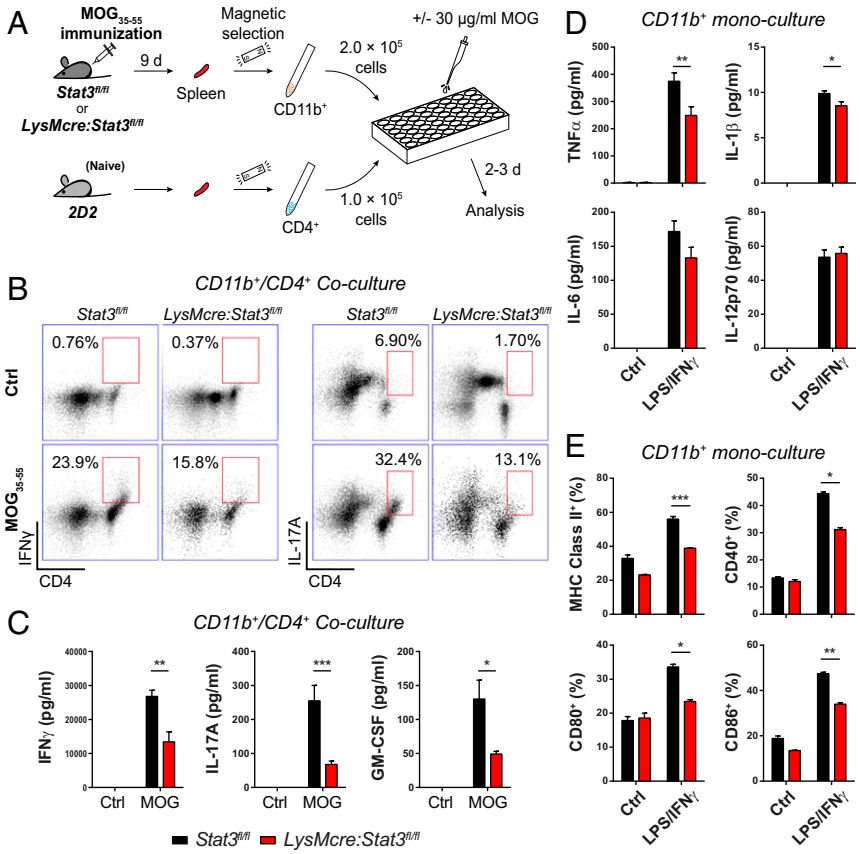

Fig. 5. CD11b$^+$ myeloid cells from mutant mice exhibit impaired capability to differentiate antigen-specific CD4$^+$ T cells ex vivo. (*A*) Schematic of the experimental design. *Stat3$^{fl/fl}$* and *LysMcre:Stat3$^{fl/fl}$* mice were immunized with MOG$_{35–55}$ and PT was not administered. After 7 to 9 d, CD11b$^+$ cells from spleens of immunized *Stat3$^{fl/fl}$* and *LysMcre:Stat3$^{fl/fl}$* mice and CD4$^+$ T cells from naive 2D2 mice were isolated with magnetic selection. CD11b$^+$ and CD4$^+$ cells were cocultured at a 2:1 ratio in the presence or absence of 30 μg/mL MOG$_{35–55}$ for 2 to 3 d before cells and the supernatant were harvested and analyzed. Cells isolated from three mice per genotype were pooled and cultured in triplicates. (*B*) The population of IFNγ- and IL-17A–producing CD4$^+$ T cells 2 d after coculturing with myeloid cells as evaluated by intracellular staining and flow cytometry. Numbers next to red boxes indicate the percentage of IFNγ$^+$ or IL-17A$^+$ cells in CD4$^+$ T cells. (*C*) The level of cytokines secreted from myeloid/T cell cocultures at div 3 as determined by multiplex immunoassay. (*D* and *E*) Production of proinflammatory cytokines and expression of antigen-presenting/costimulatory molecules by ex vivo myeloid cells. CD11b$^+$ cells isolated from immunized *LysMcre:Stat3$^{fl/fl}$* and *Stat3$^{fl/fl}$* mice as described in *A* were stimulated with or without LPS/IFNγ (10 ng/mL each) for 24 h. Production of inflammatory cytokines was measured with multiplex immunoassay (*D*), and surface expression of MHC class II, CD40, CD80, and CD86 was analyzed by flow cytometry (*E*). Data are mean ± SEM and representative of two to three independent experiments with three mice per genotype. *$P < 0.05$, **$P < 0.01$, ***$P < 0.005$.

Single-Cell Gene Profiling of Peripheral Myeloid Cells from Preclinical EAE Mice Revealed STAT3 Dependency during Cross-Activation of Myeloid Cells and Autoreactive T Cells. We have shown that peripheral myeloid cells play a critical role in antigen presentation and secretion of instructive cytokines for Th cell priming and differentiation in the EAE model of MS. In attempts to identify potential myeloid cell subsets and molecular networks that are regulated by STAT3 in an antigen-specific manner, we conducted single-cell RNA-seq (scRNA-seq) experiments on sorted CD11b$^+$ myeloid cells from *Stat3* mutant and littermate controls on day 9 post-MOG immunization (Fig. 9*A*). While a fraction of CD11b$^+$ myeloid cells underwent scRNA-seq, the remaining CD11b$^+$ cells were cocultured with naive 2D2 T cells in the presence or absence of the antigen, followed by FACS isolation and scRNA-seq (Fig. 9*A*). Two independent experiments representing six mice per genotypes generated a dataset from a total of 446 myeloid cells, of which 1,229 filtered genes were identified (Dataset S1). Unsupervised hierarchical clustering of the top 100 variably expressed genes revealed that myeloid cells organized into their respective groups and that the most variance was attributable to differences between mutant and wild-type myeloid cells that were cocultured with T cells in the presence of antigen: namely, M^{KO}/T+MOG vs. M^{WT}/T+MOG (Fig. 9*B*). In contrast, CD11b$^+$ cells freshly isolated from the spleens of mutant and wild-type mice exhibited similar gene profiles (M^{KO} ctrl vs. M^{WT} ctrl) (Fig. 9*B*), suggesting that peripheral myeloid cell development and phenotypes were similar between wild-type and *Stat3* mutant mice at the preclinical phase of EAE. A t-distributed stochastic neighbor embedding (tSNE) plot further demonstrated a close spatial relationship between clusters of mutant and wild-type myeloid cells (M^{KO} ctrl vs. M^{WT} ctrl) (Fig. 9*C*). Interestingly, in the presence of antigen and 2D2 T cells, the transcriptomic profile of *Stat3* mutant myeloid cells started to diverge substantially from that of wild-type cells on the pseudotime single-cell trajectory plot (Fig. 9*D*). These data reveal a requirement for a STAT3-dependent myeloid cell population(s) in intercellular communications that results in cross-activation of myeloid cells and antigen-specific T effector cells.

Among the top variance genes (Fig. 9*B*), the cluster of genes that were most highly expressed in the M^{KO}/T+MOG group versus others were a number of ribosomal proteins and regulatory genes related to transcription, RNA transport, and mRNA translation (e.g., *Rps19, Rps23, Rps14, Rplp2, Rpl7, Eef1a1,* and *Uba52*). The clusters of transcripts that were highly expressed in myeloid cells from the M^{WT}/T+MOG group but collapsed in *Stat3* mutant myeloid cells included genes involved in innate immune responses, antigen-presentation and processing, cytokine signaling, and inflammatory responses (e.g., *Tyrobp, Cyba, Camp, Prdx5, Fpr1, Lyz2, Ly6c, B2m, Alox5ap, Ifitm6, Ccl3,* and *Lst1*). The distribution of expression levels of several top variance transcripts in individual myeloid cells across experimental groups was visualized with violin plots (Fig. 9*E*). Of note, *Tyrobp* (DAP12), a key immunoreceptor tyrosine-based activation motif (ITAM)-bearing adaptor molecule that regulates immune responses (41), was completely down-regulated in *Stat3* mutant myeloid cells (Fig. 9*E*). Similarly, *Fcgr3* (Fc receptor γ-chain 3) was also lost in the M^{KO}/T+MOG group (Fig. 9*E*). Previous studies showed that dendritic Tyrobp- and Fc receptor γ-mediated pathways control autoimmune CD4 T cells by regulating antigen processing and presentation (42) and that *Tyrobp*-deficient mice fail to develop autoimmunity due to impaired antigen priming of T cells (43). Together, these data further support that STAT3 signaling is required for optimal APC function in the development of autoimmunity. Our results also suggest potential functional links between myeloid STAT3 and Tyrobp signaling in autoimmune diseases. Ingenuity pathway comparison analyses of gene expression profiles of the two most spatially distinct groups (M^{KO}/T+MOG vs.

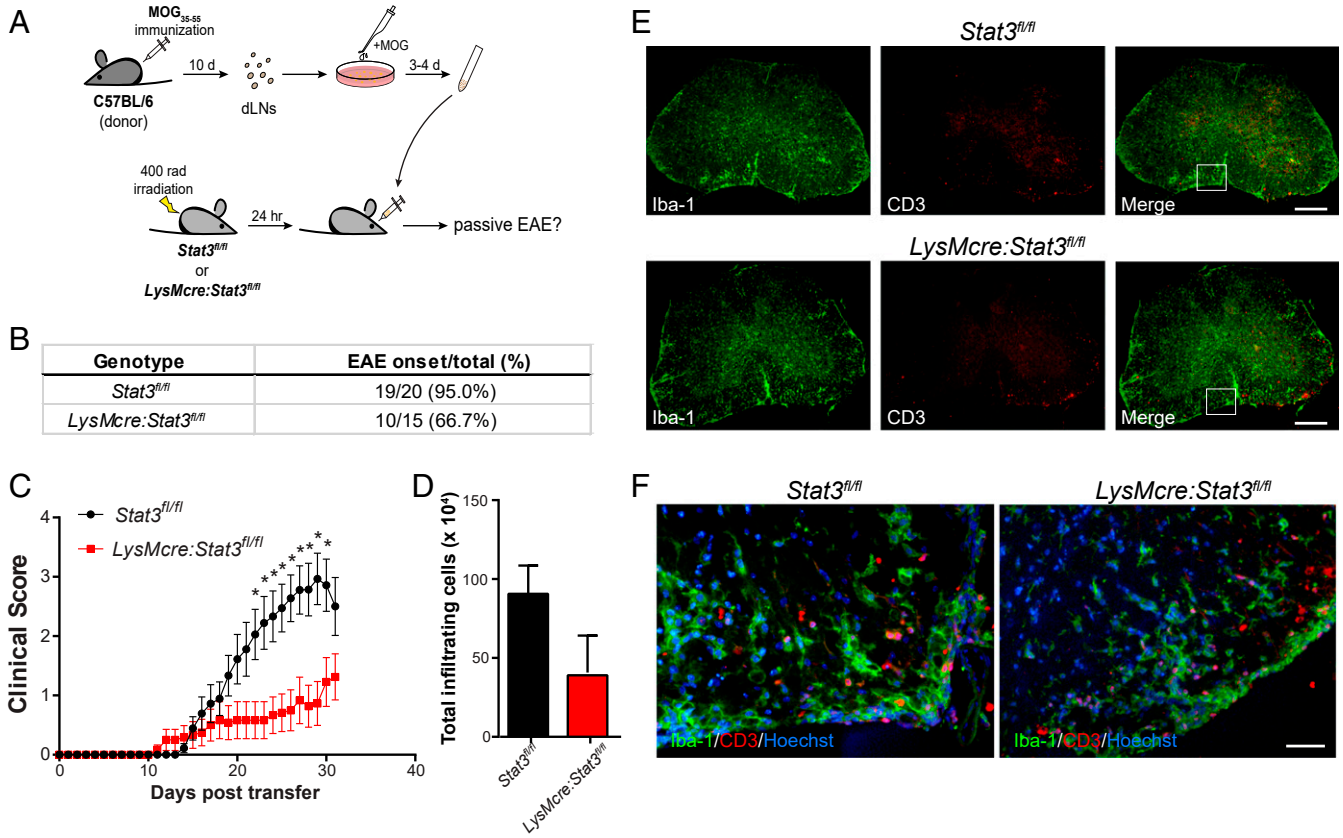

Fig. 6. *LysMcre:Stat3$^{fl/fl}$* mice are susceptible to passive EAE induced by adoptive transfer of encephalitogenic T cells. (*A*) Schematic of passive induction of EAE by adoptive transfer of encephalitogenic lymphocytes. (*B* and *C*) T cell adoptive transfer EAE was induced in *Stat3$^{fl/fl}$* ($n = 20$) and *LysMcre:Stat3$^{fl/fl}$* ($n = 15$) mice, and their clinical scores were assessed daily. Data represent mean ± SEM of five independent experiments. *$P < 0.05$. (*D*) The number of CNS infiltrating leukocytes at 30 d post-transfer (dpt). Data represent mean ± SEM of three mice per genotype. (*E* and *F*) Representative images of immunostaining of spinal cords of EAE mice with clinical scores of 2 to 2.5. Spinal cord cross-sections were immunostained for Iba-1 and CD3. Boxed areas indicate images taken at higher magnification (*F*). (Scale bars: *E*, 200 μm; *F*, 25 μm.)

M^{WT}/T+MOG) revealed that EIF2 signaling, mTOR signaling, and Fcγ receptor-mediated phagocytosis/phagosome maturation are among the top dysregulated pathways (*SI Appendix*, Fig. S13). Upstream analysis predicted RICTOR (rapamycin-insensitive companion of mTOR) as a top regulator that is inhibited in the mutant cells (activation z score −6.5, $P = 2.2 \times 10^{-42}$). RICTOR is an essential component of mammalian target of rapamycin complex 2 (mTORC2) that integrates nutrient- and growth factor-derived signals to regulate cell growth, survival and immune responses, corroborating with the general cellular functions of STAT3 and suggesting cross-talk between STAT3 and mTORC2 signaling in maintaining myeloid cell activation with MOG-specific Th cells.

Discussion

In this study, we demonstrate that STAT3 activation in peripheral myeloid cells is required for the development of CNS pathologies in an autoimmune animal model of MS. We found that phosphorylated STAT3 was significantly elevated and was frequently associated with infiltrating CD11b$^+$ cells and/or CD68$^+$ macrophages around vasculature in MS tissues. Conditional deletion of *Stat3* in myeloid cells resulted in resistance to MOG$_{35–55}$-induced EAE due to impaired encephalitogenic T cell development and suppressed leukocyte infiltration and neuroinflammation. Consistent with this hypothesis, myeloid cells isolated from immunized *LysMcre:Stat3$^{fl/fl}$* mice expressed lower levels of antigen-presenting and costimulatory molecules and were less effective in differentiating naive 2D2 CD4$^+$ T cells into Th1/Th17 effector cells. Furthermore, *LysMcre:Stat3$^{fl/fl}$* mice were susceptible to passively induced EAE. In contrast to the essential pathogenic role of peripheral myeloid STAT3 signaling, loss of CNS microglial STAT3 did not significantly affect EAE development and progression. Together, these data demonstrate a critical in vivo function of STAT3 signaling in the peripheral myeloid cell compartment in regulating encephalitogenic T cell development and neuroinflammation.

The main mechanism by which STAT3 inactivation in peripheral myeloid cells abolished the development of EAE is impaired functions of myeloid APCs in priming and differentiating CD4$^+$ T cells into encephalitogenic T cells in vivo. *Stat3* ablation in myeloid cells did not alter circulating or splenic myeloid cell populations at preclinical stages, as determined by immunophenotyping and myeloid cell gene profiling. However, the functionality of these *Stat3* mutant and WT myeloid cells differed drastically when they interacted with autoreactive CD4$^+$ T cells in the presence of a cognate antigen. In contrast to WT myeloid cells, *Stat3* mutant myeloid cells were ineffective in priming and differentiating naive CD4$^+$ T cells into Th1/Th17 cells ex vivo, resulting in lower Th1/Th17 cytokine secretion (IL-17, IFNγ, and GM-CSF) that in turn led to less monocyte activation and lower production of proinflammatory cytokines (IL-1β, TNF, IL-12, IL-23, and IL-6). Indeed, CD11b$^+$CD11c$^+$ APCs were found at reduced frequencies in MOG-stimulated cocultures of mutant myeloid cells/T cells as compared to WT counterparts. Our results thus reveal a previously unrecognized role for myeloid STAT3 signaling in modulating antigen-dependent interactions

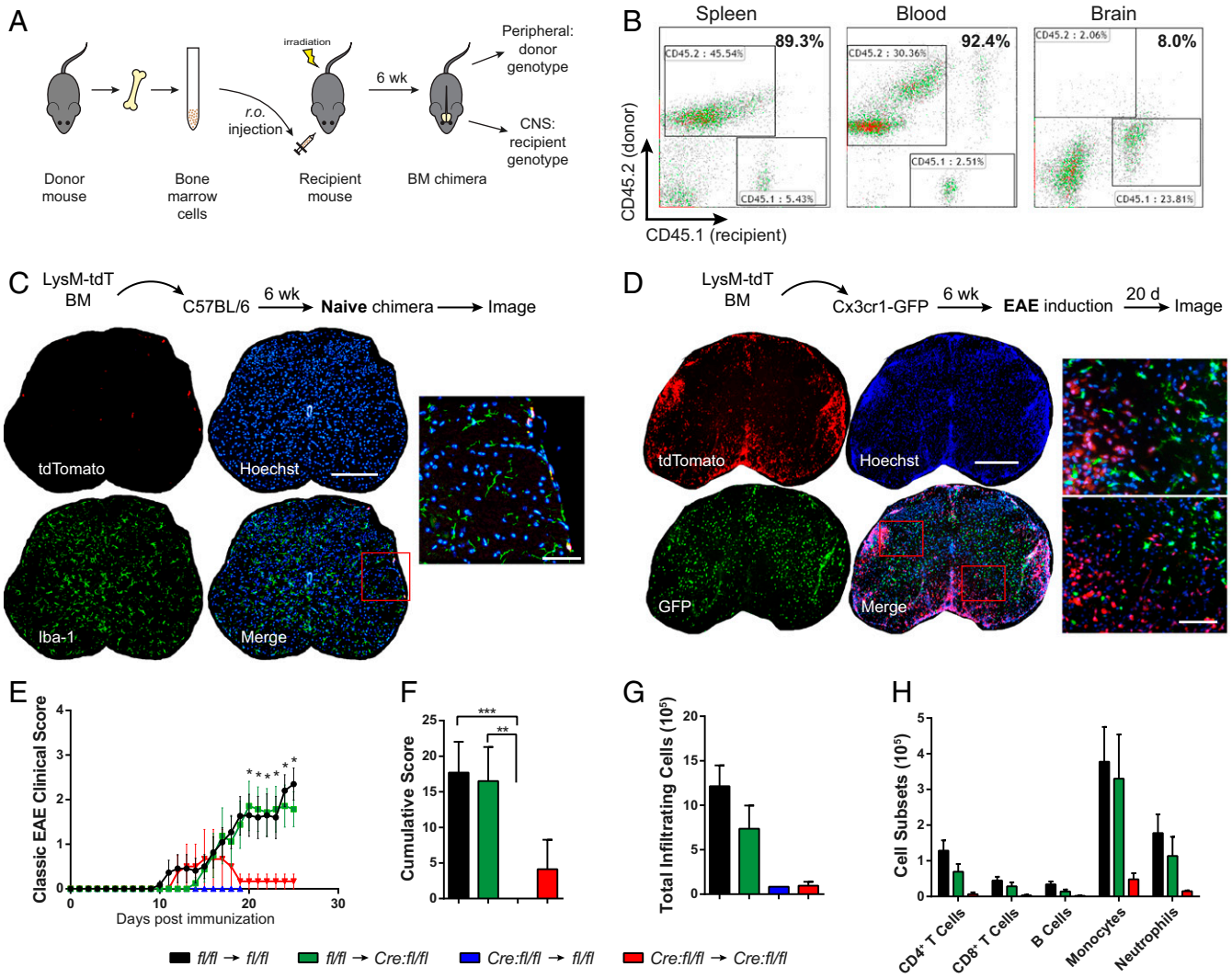

Fig. 7. STAT3 activation in the peripheral myeloid cells, but not CNS myeloid cells, is required for MOG_{35-55}-induced EAE. (*A*) Schematic of experimental design of bone marrow chimeric experiments. (*B*) Efficacy of BM engraftment in congenic recipients. Engraftment of CD45.1 BM cells into irradiated CD45.2 congenic C57BL/6 mice (CD45.1 → CD45.2) was analyzed 6 wk after BM transplantation. Mononuclear cells from spleen, blood, and the CNS of chimeric mice were stained with antibodies against CD45.1 and CD45.2 and analyzed by flow cytometry. Data are representative of four to eight chimera. (*C*) Representative spinal cord images of naive chimera reconstituted with BM from *LysMcre:Rosa-tdTomato* reporter mice. There was minimal CNS engraftment by donor myeloid cells in unchallenged chimeric mice 6 to 9 wk after transplantation ($n = 3$). (Scale bars: whole cross section, 500 μm; *Inset*, 50 μm.) *Insets*, magified areas in red boxed highlighting double-positive cells. (*D*) Representative images of dual reporter chimera at the peak of EAE, illustrating massive infiltrating *LysM*-driven tdTomato$^+$ myeloid cells at inflamed loci, clearly distinguishable from resident microglia (GFP$^+$). No overlap between tdTomato and GFP was observed ($n = 2$). (*E* and *F*) Mean EAE clinical scores and cumulative scores of *Stat3* chimeric mice. Active EAE was induced in chimeric mice 6 wk post-BM engraftment and scored daily. *Stat3*$^{fl/fl}$ (BM donor) → *Stat3*$^{fl/fl}$ (recipient), $n = 11$ mice; *Stat3*$^{fl/fl}$ → *LysMcre:Stat3*$^{fl/fl}$, $n = 8$; *LysMcre:Stat3*$^{fl/fl}$ → *Stat3*$^{fl/fl}$, $n = 11$; *LysMcre:Stat3*$^{fl/fl}$ → *LysMcre:Stat3*$^{fl/fl}$, $n = 4$. (*G* and *H*) Infiltrating leukocytes were isolated from the CNS of EAE mice at 26 dpi, immunolabeled, and analyzed with flow cytometry. Data represent mean ± SEM; $^*P < 0.05$, $^{**}P < 0.01$, $^{***}P < 0.005$.

with CD4$^+$ T cells, as well as a cytokine environment that drives autoimmune inflammation.

Myeloid cells are heterogeneous and phenotypically dynamic at different activation stages in terms of surface protein profiles, signaling molecule expression and cytokine production. Using a high-dimensional single-cell mass cytometry approach, a recent study systematically compared myeloid cell populations across different clinical stages of EAE and identified five separate clusters of peripherally derived, CNS-infiltrating myeloid cells (44). Interestingly, among these, two monocyte populations had increased pSTAT3 signal at the onset of EAE, compared to all other infiltrating monocytes or CNS-resident myeloid cells, and most likely represented activated myeloid APCs based on their surface marker expression patterns (44). These findings are in accordance with our data demonstrating that selective inactivation of STAT3 signaling in peripheral myeloid cells ameliorates the development of encephalitogenic T cells and EAE. Our study also highlights the potential of myeloid STAT3 as a therapeutic target in autoimmune demyelinating disease. Single-cell transcriptome profiling of myeloid cells revealed that the STAT3-dependent impairment only becomes evident when myeloid cells were cocultured with MOG-reactive T cells, suggesting yet-to-be-identified STAT3-dependent, antigen-initiated reciprocal communications between CD4$^+$ T cells and myeloid cells that drive CNS inflammation. In line with these findings, loss of MHC class II expression on CD11c$^+$ myeloid cells effectively prevented EAE induction (45). The exact nature of activated myeloid cells that are regulated by STAT3 signaling in the context of EAE and T cell activation remains to be determined and likely

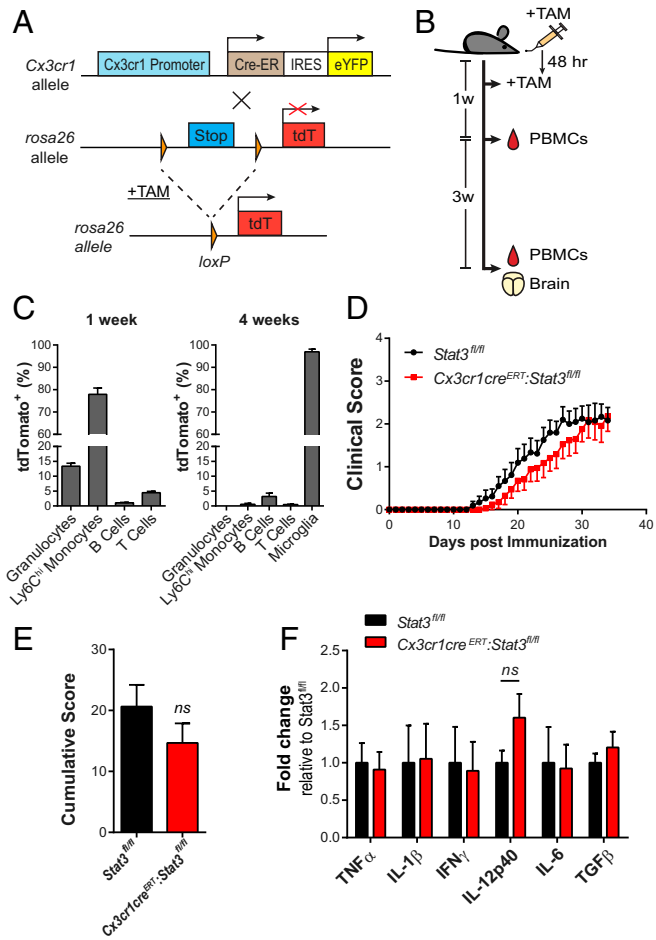

Fig. 8. STAT3 signaling in microglia is dispensable for EAE induction and progression. (*A*) Generation of tamoxifen-inducible *Cx3cr1*-Cre reporter mice (*Cx3cr1*^{CreERT}*:Rosa-tdT*). Tamoxifen (TAM) administration enables Cre-dependent removal of the Stop cassette of the Rosa26-tdTomato allele, allowing the expression of tdTomato in targeted cells. IRES, internal ribosome entry site; eYFP, enhanced yellow fluorescent protein. (*B* and *C*) *Cx3cr1*^{CreERT}*:Rosa-tdT* mice (n = 3) were given tamoxifen at age of 5 wk. tdTomato expression in peripheral blood mononuclear cells (PBMCs) 1 and 4 wk after TAM and in CNS mononuclear cells 4 wk after TAM was analyzed by flow cytometry. Granulocytes, CD11b$^+$Gr-1$^+$; Ly6C^{hi} monocytes, CD11b$^+$Ly6C^{hi}; T cells, CD3$^+$; B cells, CD19$^+$; microglia, CD11b$^+$CD45^{int}. (*D*–*F*) *Cx3cr1*^{CreERT}*:Stat3*$^{fl/fl}$ (n = 17) and *Stat3*$^{fl/fl}$ mice (n = 21) were treated with tamoxifen. EAE was induced 4 wk later and assessed daily. Mean EAE clinical scores (*D*), cumulative scores up to 30 dpi (*E*), and quantitative RT-PCR analyses of cytokines from spinal cord tissues at 30 dpi (*F*). Data represent mean ± SEM of fold changes relative to *Stat3*$^{fl/fl}$. *Stat3*$^{fl/fl}$, n = 8; *Cx3cr1*^{CreERT}*:Stat3*$^{fl/fl}$, n = 6. ns, not significant.

requires a combination of functional and transcriptomic analyses at single-cell levels.

Besides regulating APC functions in activating MOG-specific T cells in vivo and ex vivo, STAT3 signaling in peripheral myeloid cells also affects the effector phase of EAE as *LysMcre:Stat3*$^{fl/fl}$ mice developed passive EAE at lower incidence and severity than their littermate controls. Neutrophils have been shown to be essential in the early phase of EAE and may also contribute to MS pathogenesis (46, 47). Although they have not been shown to directly induce CD4$^+$ T cell differentiation, infiltrating neutrophils secrete inflammatory molecules that promote local APC activation, which in turn reactivates myelin-specific T cells ensuring neuroinflammation (48). Neutrophils may acquire APC-like properties and influence antigen-specific T cell functions as recent evidence suggests that neutrophils have the capacity to function as antigen-presenting cells under certain pathological conditions (49). Whether this occurs in EAE and whether STAT3 regulates potential APC-like functions of neutrophils are presently open questions. Deletion of *Socs3,* an inducible negative regulator of STAT3, in myeloid cells resulted in a more severe form of atypical EAE that was mainly mediated by enhanced neutrophil functions (36, 50). Although we did not observe significant differences in neutrophil populations between *Stat3* mutant and control mice at preclinical and EAE onset or between wild-type and mutant ex vivo myeloid cells cocultured with 2D2 T cells, we did, however, find a significant reduction in antigen-dependent MPO secretion in the mutant CD11b$^+$ cells plus 2D2 cocultures (*SI Appendix*, Fig. S10*B*). MPO is mainly secreted from activated neutrophils and has been implicated in myeloid cell infiltration and blood–brain barrier (BBB) breakage during EAE (51). In addition, our pathway analysis of the myeloid cell RNA-seq dataset suggests decreased fMLP signaling in neutrophils, IL-8/CXCL8 signaling, and leukocyte extravasation pathways in *Stat3* mutant myeloid cells (*SI Appendix*, Fig. S13). Immune cell extravasation across the BBB into the CNS parenchyma represents a critical step in breaking CNS immune privilege and initiating neuroinflammatory reactions. Matrix metalloproteinases (MMPs) such as MMP-2/9, secreted primarily by infiltrated myeloid cells have been shown to degrade the basement membrane matrix and promote leukocyte diapedesis (52). Interestingly, MMP-8, produced mainly by infiltrating neutrophils during EAE and of which gene ablation reduces EAE progression (53), was down-regulated in *Stat3* mutant myeloid cell populations only when stimulated with antigen cognate T cells (Fig. 9*E*). These findings suggest that STAT3 signaling in granulocytes likely contributes to leukocyte transmigration and activation during CNS autoimmune pathogenesis.

We found increased STAT3 activation in infiltrating myeloid cells in the vicinity of blood vessels in apparent newly forming MS lesions. The *STAT3* locus has been associated with two autoimmune diseases: Crohn's disease and MS (54). Comorbidity of inflammatory bowel disease and MS has been implicated in some MS patients (55). Interestingly, a *STAT3* allele variant associated with a protective haplotype in MS is associated with increased risk in Crohn's disease (24). Animal studies showed that targeted deletion of *Stat3* in CD4 T cells (30) and myeloid cells (the current study) prevents the development of EAE and that pharmacological inhibition of JAK/STAT ameliorates EAE pathogenesis and progression (31). These studies collectively support a significant role for STAT3 in autoimmune disease pathogenesis. One limitation of this study is that *LysMcre:Stat3*$^{fl/-}$ mice were prone to developing chronic enterocolitis with age with enhanced IL-12p40 production and Th1 activity (39, 56). The inflamed gastrointestinal tract could disrupt the balance of commensal microbiota that may affect EAE and other autoimmune diseases (57). Although a few of our mutant mice developed rectal prolapse during or before EAE induction, we did not observe any correlations between these two phenotypes as all *Stat3* mutant mice failed to develop EAE and mutant mice reconstituted with wild-type marrows were fully susceptible to active EAE. Moreover, mutant mice with rectal prolapse developed passive EAE after adoptive transfer of encephalitogenic T cells. It is noteworthy that IL-10–deficient mice also develop chronic enterocolitis (58). However, unlike *lysMCre:Stat3*$^{fl/fl}$ mice, IL-10–deficient mice are more susceptible to EAE and develop more severe symptoms (32). This suggests that resistance of myeloid *Stat3* mutant mice to active EAE is unlikely simply due to their predisposition to developing enterocolitis and cannot be solely explained by potential effects on commensal microbiota. Moreover, myeloid cells isolated from immunized mutant mice exhibited impaired, rather than enhanced, functions in priming MOG-specific CD4$^+$ T cells.

In summary, our data suggest that STAT3 activation in monocytic cells is a feature of active MS lesions. Our data also demonstrate a previously uncharacterized, but essential, pathogenic

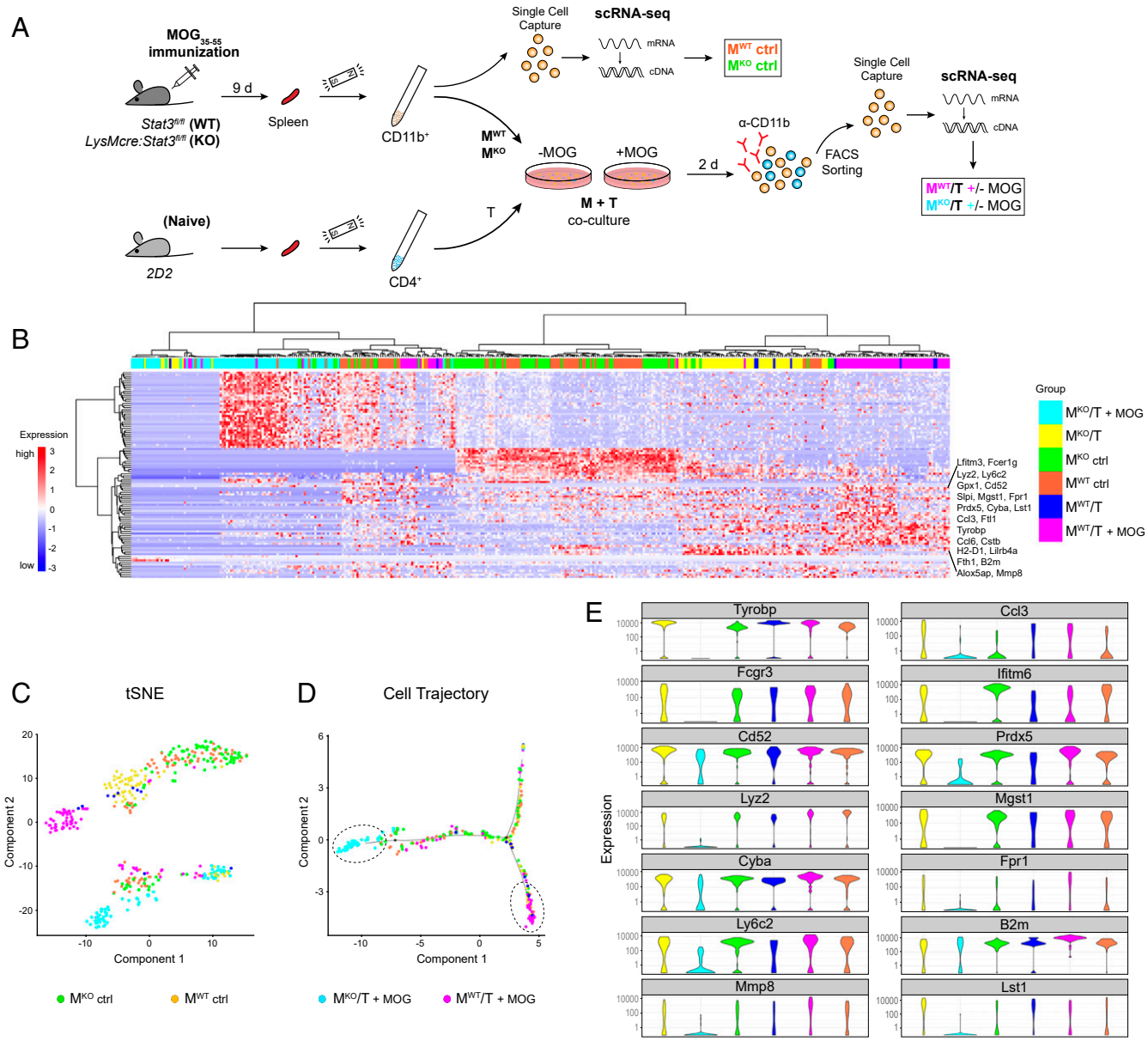

Fig. 9. Single-cell RNA-seq of ex vivo myeloid cells reveals a requirement for myeloid STAT3 in activation of T helper cells. (*A*) Experimental design for single-cell gene profiling of ex vivo myeloid cells from preclinical EAE mice and of sorted myeloid cells after coculturing with naive 2D2 T cells in the absence and presence of cognate antigen $MOG_{35–55}$. (*B*) Heat map of unsupervised clustering of top 100 variable genes across all single $CD11b^+$ cells and treatment conditions. Data are representative of six mice per genotype from two independent experiments. (*C*) tSNE representation of individual myeloid cells in each experimental group as measured by scRNA-seq and Monocle clustering. Each dot represents an individual cell. (*D*) Pseudotime single-cell trajectory plot of individual myeloid cells from all groups showing that *Stat3* mutant myeloid cells were transitioned into a most distant state from that of WT myeloid cells after cognate MOG activation with Th cells. (*E*) Violin plots showing the distribution of expression levels of indicated genes across myeloid cells as grouped by genotypes and treatment conditions. KO, knockout.

role for STAT3 signaling in myeloid cells in the development of CNS autoimmunity in experimental models of MS. Our results reveal a regulatory capacity of STAT3 in myeloid APC functions and in sustaining cognate antigen-dependent cross-activation of myeloid cells and T helper cells that drives autoimmune-mediated demyelination. This study implies that targeting the JAK/STAT3 axis in the myeloid compartment may be beneficial in curbing inflammatory demyelinating diseases.

Methods

Human Brain Tissues. Postmortem brain tissues (*SI Appendix*, Table S1) from clinical diagnosed and neuropathologically confirmed MS and control cases were processed and characterized as described previously (59).

Animals. *Stat3*$^{fl/fl}$ mice containing two LoxP sites flanking exon 22 that encodes the tyrosine residue (Y705) essential for STAT3 activation (39) were backcrossed to C57BL/6 mice for at least nine generations (60). All mice were housed under constant 12-h light/dark cycles in covered cages and fed with a standard rodent diet ad libitum under specific pathogen-free conditions at the Comparative Medicine Program, Texas A&M University. Animal studies were approved by the Institutional Animal Care and Use Committee.

Detailed methods can be found in *SI Appendix*.

Data Availability Statement. The sequence reported in this paper has been deposited in the National Center for Biotechnology Information (NCBI) BioProject database (accession no. PRJNA605403).

ACKNOWLEDGMENTS. We thank Drs. Shizuo Akira (Osaka University, Japan) and John DiGiovanni (University of Texas Anderson Cancer Center) for providing the Stat3^{flox} mice; Dr. Gus Wright for assistance in FACS of myeloid cells; and Dr. Michael Deveau and Ms. Linda Knight for mouse irradiation. Human tissue specimens were kindly provided by the Rocky Mountain MS Center (supported by the National Multiple Sclerosis Society), and the Human Brain and Spinal Fluid Resource Center of the Veterans Affairs West Los Angeles Healthcare Center (sponsored by the National Institute of Neurological Disorders and Stroke, National Institute of Mental Health, the National Multiple Sclerosis Society, and the Department of Veterans Affairs). This study was funded in part by National Institutes of Health Grant R01NS060017 and National Multiple Sclerosis Society Grants RG3975 and RG1507 (to J.L.).

1. M. Sospedra, R. Martin, Immunology of multiple sclerosis. *Annu. Rev. Immunol.* **23**, 683–747 (2005).
2. W. Brück *et al*., Monocyte/macrophage differentiation in early multiple sclerosis lesions. *Ann. Neurol.* **38**, 788–796 (1995).
3. A. Compston, A. Coles, Multiple sclerosis. *Lancet* **372**, 1502–1517 (2008).
4. M. K. Mishra, V. W. Yong, Myeloid cells–targets of medication in multiple sclerosis. *Nat. Rev. Neurol.* **12**, 539–551 (2016).
5. M. Mitrovič *et al*.; International Multiple Sclerosis Genetics Consortium; International Multiple Sclerosis Genetics Consortium, Low-frequency and rare-coding variation contributes to multiple sclerosis risk. *Cell* **175**, 1679–1687.e7 (2018).
6. L. Bö *et al*., Detection of MHC class II-antigens on macrophages and microglia, but not on astrocytes and endothelia in active multiple sclerosis lesions. *J. Neuroimmunol.* **51**, 135–146 (1994).
7. A. P. Henderson, M. H. Barnett, J. D. Parratt, J. W. Prineas, Multiple sclerosis: Distribution of inflammatory cells in newly forming lesions. *Ann. Neurol.* **66**, 739–753 (2009).
8. J. A. Hollenbach, J. R. Oksenberg, The immunogenetics of multiple sclerosis: A comprehensive review. *J. Autoimmun.* **64**, 13–25 (2015).
9. A. Achiron, M. Gurevich, N. Friedman, N. Kaminski, M. Mandel, Blood transcriptional signatures of multiple sclerosis: Unique gene expression of disease activity. *Ann. Neurol.* **55**, 410–417 (2004).
10. R. Ratzer *et al*., Gene expression analysis of relapsing-remitting, primary progressive and secondary progressive multiple sclerosis. *Mult. Scler.* **19**, 1841–1848 (2013).
11. E. H. Tran, K. Hoekstra, N. van Rooijen, C. D. Dijkstra, T. Owens, Immune invasion of the central nervous system parenchyma and experimental allergic encephalomyelitis, but not leukocyte extravasation from blood, are prevented in macrophage-depleted mice. *J. Immunol.* **161**, 3767–3775 (1998).
12. S. Agrawal *et al*., Dystroglycan is selectively cleaved at the parenchymal basement membrane at sites of leukocyte extravasation in experimental autoimmune encephalomyelitis. *J. Exp. Med.* **203**, 1007–1019 (2006).
13. M. Greter *et al*., Dendritic cells permit immune invasion of the CNS in an animal model of multiple sclerosis. *Nat. Med.* **11**, 328–334 (2005).
14. L. Izikson, R. S. Klein, I. F. Charo, H. L. Weiner, A. D. Luster, Resistance to experimental autoimmune encephalomyelitis in mice lacking the CC chemokine receptor (CCR)2. *J. Exp. Med.* **192**, 1075–1080 (2000).
15. B. T. Fife, G. B. Huffnagle, W. A. Kuziel, W. J. Karpus, CC chemokine receptor 2 is critical for induction of experimental autoimmune encephalomyelitis. *J. Exp. Med.* **192**, 899–905 (2000).
16. B. Ajami, J. L. Bennett, C. Krieger, K. M. McNagny, F. M. V. Rossi, Infiltrating monocytes trigger EAE progression, but do not contribute to the resident microglia pool. *Nat. Neurosci.* **14**, 1142–1149 (2011).
17. S. Hucke *et al*., Licensing of myeloid cells promotes central nervous system autoimmunity and is controlled by peroxisome proliferator-activated receptor γ. *Brain* **135**, 1586–1605 (2012).
18. I. Bartholomäus *et al*., Effector T cell interactions with meningeal vascular structures in nascent autoimmune CNS lesions. *Nature* **462**, 94–98 (2009).
19. P. Kivisäkk *et al*., Localizing central nervous system immune surveillance: Meningeal antigen-presenting cells activate T cells during experimental autoimmune encephalomyelitis. *Ann. Neurol.* **65**, 457–469 (2009).
20. I. L. King, T. L. Dickendesher, B. M. Segal, Circulating Ly-6C+ myeloid precursors migrate to the CNS and play a pathogenic role during autoimmune demyelinating disease. *Blood* **113**, 3190–3197 (2009).
21. J. J. O'Shea, P. J. Murray, Cytokine signaling modules in inflammatory responses. *Immunity* **28**, 477–487 (2008).
22. S. Sawcer *et al*.; International Multiple Sclerosis Genetics Consortium; Wellcome Trust Case Control Consortium 2, Genetic risk and a primary role for cell-mediated immune mechanisms in multiple sclerosis. *Nature* **476**, 214–219 (2011).
23. S. E. Baranzini *et al*.; GeneMSA Consortium, Pathway and network-based analysis of genome-wide association studies in multiple sclerosis. *Hum. Mol. Genet.* **18**, 2078–2090 (2009).
24. E. Jakkula *et al*., Genome-wide association study in a high-risk isolate for multiple sclerosis reveals associated variants in STAT3 gene. *Am. J. Hum. Genet.* **86**, 285–291 (2010).
25. C. M. Lill *et al*., Independent replication of STAT3 association with multiple sclerosis risk in a large German case-control sample. *Neurogenetics* **13**, 83–86 (2012).
26. G. Frisullo *et al*., The effect of disease activity on leptin, leptin receptor and suppressor of cytokine signalling-3 expression in relapsing-remitting multiple sclerosis. *J. Neuroimmunol.* **192**, 174–183 (2007).
27. E. Canto, N. Isobe, A. Didonna, S. L. Hauser, J. R. Oksenberg; MS-EPIC Study Group, Aberrant STAT phosphorylation signaling in peripheral blood mononuclear cells from multiple sclerosis patients. *J. Neuroinflammation* **15**, 72 (2018).
28. G. Frisullo *et al*., pSTAT1, pSTAT3, and T-bet expression in peripheral blood mononuclear cells from relapsing-remitting multiple sclerosis patients correlates with disease activity. *J. Neurosci. Res.* **84**, 1027–1036 (2006).
29. J. Q. Lu, C. Power, G. Blevins, F. Giuliani, V. W. Yong, The regulation of reactive changes around multiple sclerosis lesions by phosphorylated signal transducer and activator of transcription. *J. Neuropathol. Exp. Neurol.* **72**, 1135–1144 (2013).
30. X. Liu, Y. S. Lee, C.-R. Yu, C. E. Egwuagu, Loss of STAT3 in CD4+ T cells prevents development of experimental autoimmune diseases. *J. Immunol.* **180**, 6070–6076 (2008).
31. Y. Liu *et al*., Therapeutic efficacy of suppressing the Jak/STAT pathway in multiple models of experimental autoimmune encephalomyelitis. *J. Immunol.* **192**, 59–72 (2014).
32. E. Bettelli *et al*., IL-10 is critical in the regulation of autoimmune encephalomyelitis as demonstrated by studies of IL-10- and IL-4-deficient and transgenic mice. *J. Immunol.* **161**, 3299–3306 (1998).
33. H.-P. Eugster, K. Frei, M. Kopf, H. Lassmann, A. Fontana, IL-6-deficient mice resist myelin oligodendrocyte glycoprotein-induced autoimmune encephalomyelitis. *Eur. J. Immunol.* **28**, 2178–2187 (1998).
34. E. B. Samoilova, J. L. Horton, B. Hilliard, T. S. T. Liu, Y. Chen, IL-6-deficient mice are resistant to experimental autoimmune encephalomyelitis: Roles of IL-6 in the activation and differentiation of autoreactive T cells. *J. Immunol.* **161**, 6480–6486 (1998).
35. Y. Okuda *et al*., IL-6 plays a crucial role in the induction phase of myelin oligodendrocyte glucoprotein 35-55 induced experimental autoimmune encephalomyelitis. *J. Neuroimmunol.* **101**, 188–196 (1999).
36. H. Qin *et al*., Signal transducer and activator of transcription-3/suppressor of cytokine signaling-3 (STAT3/SOCS3) axis in myeloid cells regulates neuroinflammation. *Proc. Natl. Acad. Sci. U.S.A.* **109**, 5004–5009 (2012).
37. K. Takeda *et al*., Stat3 activation is responsible for IL-6-dependent T cell proliferation through preventing apoptosis: Generation and characterization of T cell-specific Stat3-deficient mice. *J. Immunol.* **161**, 4652–4660 (1998).
38. E. Bettelli *et al*., Myelin oligodendrocyte glycoprotein-specific T cell receptor transgenic mice develop spontaneous autoimmune optic neuritis. *J. Exp. Med.* **197**, 1073–1081 (2003).
39. K. Takeda *et al*., Enhanced Th1 activity and development of chronic enterocolitis in mice devoid of Stat3 in macrophages and neutrophils. *Immunity* **10**, 39–49 (1999).
40. C. N. Parkhurst *et al*., Microglia promote learning-dependent synapse formation through brain-derived neurotrophic factor. *Cell* **155**, 1596–1609 (2013).
41. I. R. Turnbull, M. Colonna, Activating and inhibitory functions of DAP12. *Nat. Rev. Immunol.* **7**, 155–161 (2007).
42. D. B. Graham *et al*., ITAM signaling in dendritic cells controls T helper cell priming by regulating MHC class II recycling. *Blood* **116**, 3208–3218 (2010).
43. A. B. Bakker *et al*., DAP12-deficient mice fail to develop autoimmunity due to impaired antigen priming. *Immunity* **13**, 345–353 (2000).
44. B. Ajami *et al*., Single-cell mass cytometry reveals distinct populations of brain myeloid cells in mouse neuroinflammation and neurodegeneration models. *Nat. Neurosci.* **21**, 541–551 (2018).
45. M. J. C. Jordão *et al*., Single-cell profiling identifies myeloid cell subsets with distinct fates during neuroinflammation. *Science* **363**, eaat7554 (2019).
46. T. Woodberry, S. E. Bouffler, A. S. Wilson, R. L. Buckland, A. Brüstle, The emerging role of neutrophil granulocytes in multiple sclerosis. *J. Clin. Med.* **7**, 511 (2018).
47. J. M. Rumble *et al*., Neutrophil-related factors as biomarkers in EAE and MS. *J. Exp. Med.* **212**, 23–35 (2015).
48. K. Steinbach, M. Piedavent, S. Bauer, J. T. Neumann, M. A. Friese, Neutrophils amplify autoimmune central nervous system infiltrates by maturing local APCs. *J. Immunol.* **191**, 4531–4539 (2013).
49. S. Costa, D. Bevilacqua, M. A. Cassatella, P. Scapini, Recent advances on the crosstalk between neutrophils and B or T lymphocytes. *Immunology* **156**, 23–32 (2019).
50. Z. Yan *et al*., Deficiency of Socs3 leads to brain-targeted experimental autoimmune encephalomyelitis via enhanced neutrophil activation and ROS production. *JCI Insight* **4**, e126520 (2019).
51. H. Zhang *et al*., Inhibition of myeloperoxidase at the peak of experimental autoimmune encephalomyelitis restores blood-brain barrier integrity and ameliorates disease severity. *J. Neurochem.* **136**, 826–836 (2016).
52. H. Toft-Hansen, R. K. Nuttall, D. R. Edwards, T. Owens, Key metalloproteinases are expressed by specific cell types in experimental autoimmune encephalomyelitis. *J. Immunol.* **173**, 5209–5218 (2004).
53. A. R. Folgueras *et al*., Collagenase-2 deficiency or inhibition impairs experimental autoimmune encephalomyelitis in mice. *J. Biol. Chem.* **283**, 9465–9474 (2008).
54. C. Cotsapas, M. Mitrovic, Genome-wide association studies of multiple sclerosis. *Clin. Transl. Immunology* **7**, e1018 (2018).
55. M. Kosmidou *et al*., Multiple sclerosis and inflammatory bowel diseases: A systematic review and meta-analysis. *J. Neurol.* **264**, 254–259 (2017).
56. M. Kobayashi *et al*., Toll-like receptor-dependent production of IL-12p40 causes chronic enterocolitis in myeloid cell-specific Stat3-deficient mice. *J. Clin. Invest.* **111**, 1297–1308 (2003).
57. N. Kamada, S. U. Seo, G. Y. Chen, G. Núñez, Role of the gut microbiota in immunity and inflammatory disease. *Nat. Rev. Immunol.* **13**, 321–335 (2013).
58. R. Kühn, J. Löhler, D. Rennick, K. Rajewsky, W. Müller, Interleukin-10-deficient mice develop chronic enterocolitis. *Cell* **75**, 263–274 (1993).
59. S. Kim, A. J. Steelman, Y. Zhang, H. C. Kinney, J. Li, Aberrant upregulation of astroglial ceramide potentiates oligodendrocyte injury. *Brain Pathol.* **22**, 41–57 (2012).
60. A. J. Steelman *et al*., Activation of oligodendroglial Stat3 is required for efficient remyelination. *Neurobiol. Dis.* **91**, 336–346 (2016).